https://doi.org/10.1007/s12583-021-1556-2

The interpretation of seismogenic fault of the Maduo Mw 7.3 Earthquake, Qinghai based on remote sensing images——a branch of the East Kunlun fault system

Guanghao Ha[1], Jinrui Liu[1], Zhikun Ren[1*], Xiaoxiao Zhu[1], Guodong Bao[1], Dengyun Wu[1], Zhiliang Zhang[1]

1 Key laboratory of Seismic and Volcanic Hazards, Institute of Geology, China Earthquake Administration, Beijing 100029, China

Abstract: On May 22, 2021, a Mw 7.3 earthquake occurred in Maduo County, Qinghai Province with the epicenter of 34.59°N~98.34°E. The distribution of aftershocks and surface ruptures suggested that the seimogenic fault might be the Jiangcuo fault (JF), ~70 km south of East Kunlun fault (EKLF). Due to the high altitude and sparse human habitats, there are very few researches on the Jiangcuo fault, which makes us know little about the the deformation features and even the geometry of Jiangcuo fault. In this study, we used the high-resolution pre-earthquake satellite images to interpret the spatial distribution and geometry of the Jiangcuo fault. Our results show that the Jiangcuo fault strikes nearly east, extending 180-km-long from Eling lake to east of Changmahe Town. Based on the geometric features, the Jiangcuo fault could be divided into three segments characterized as the linear structures, fault valleys, scarps and systematic offset of channels. The boundary between Bayan Har block and Qaidam block is presented as a wide deformation zone named of Kunlun belt that is composed of East Kunlun fault and several branch faults around Anemaqen Mountain. Geometric analysis and deep lithosphere structure around Maduo County suggest that the Jiangcuo fault should be one of branch of East Kunlun fault at south, where the Kunlun fault developed as a giant flower structure. In addition, the seismic hazards potential of Jiangcuo fault should be given enough attention in the future, because west of the Jiangcuo Fault, there is a rupture gap between the co-seismic surface ruptures of the 2001 Kunlun, 2021 Maduo and 1937 Huashixia earthquakes.

** Corresponding author: rzk@ies.ac.cn
Key laboratory of Seismic and Volcanic Hazards, Institute of Geology, China Earthquake Administration

Key words: Jiangcuo fault, seismogenic fault, East Kunlun fault, Maduo earthquake, Rupture gap

0 Introduction

A Mw 7.3 earthquake attacked Maduo, Qinghai Province on May 22, 2021 according to China Earthquake Networks Center with the epicenter of 34.59°N, 98.34°E. The Maduo earthquake is located at central Tibetan plateau, interior of the Bayan Har block (BH), around which many strong earthquakes ($M>7.0$) occurred, such as the 1937 Huashixia Mw 7.5, 1997 Manyi Mw 7.5, 2001 Kunlun Mw 7.8, 2008 Wenchuan Mw 7.9, 2010 Yushu Mw 6.9, 2014 Mw 7.2 Yutian earthquakes etc. (Fig. 1). The distribution of aftershocks and surface ruptures indicate that the seismogenic fault should be the NW-trending left-lateral strike-slip Jiangcuo fault (JF), eastern segment of Kunlun Shankou-Jiangcuo fault (KSJF, Fig. 1; Li Z. et al., 2021; Pan et al., 2021; Wang et al., 2021). Previous strong earthquakes around Bayan Har block mainly occurred along the main boundary faults, e.g. the 1937 Huashixia M 7.5, the 2001 Kunlun Mw 7.8, the 1997 Manyi Mw 7.5 and the 2008 Wenchuan Mw 7.9 earthquakes. However, the Maduo earthquake occurred along Jiangcuo fault, ~70 km south of the East Kunlun fault (Fig. 1). It is a debate that whether the Jiangcuo fault is a branch of East Kunlun fault or a secondary fault within the block, which is important for understanding regional deformation pattern as well as the seismic hazard assessment. For different cognitions of the tectonic attribute of Jiangcuo fault, we would have different understandings of the deformation models and seismic risk analysis of Bayan Har block. Due to the high altitude, rare human habitats and difficulties in access to this region, we knew little about the Jiangcuo fault. Zhang et al. (1996) first reported the Holocene activity of Jiangcuo fault. However, the detailed parameters of Jiangcuo fault, e.g. spatial distributions, geometric features, offset landforms, were not available.

More recently, technologies that enable acquisition of high-resolution satellite image (e.g., WorldView, Pleiades and GF-1/2) have become increasingly available. These technologies not only provided an opportunity to map the seismic surface ruptures after a strong earthquake, e.g., 2001 Kunlun earthquake (Lin et al., 2011), 1997 Manyi earthquake (Ren and Zhang, 2019), but also brought significant advances in the ability to recognize the fault trace and geomorphic offsets along active faults. In this paper, we used high-resolution satellite images (<1 m) to interpret the fault trace and typical displaced landforms of Jiangcuo fault. Together with previous deep reflection seismic profile in the adjacent regions, we finally discussed the 3D seismogenic structures of the Maduo earthquake. We proposed that the Jiangcuo fault is a left-laterally dominated strike-slip fault, which is also a sub-branch of the East Kunlun fault zone.

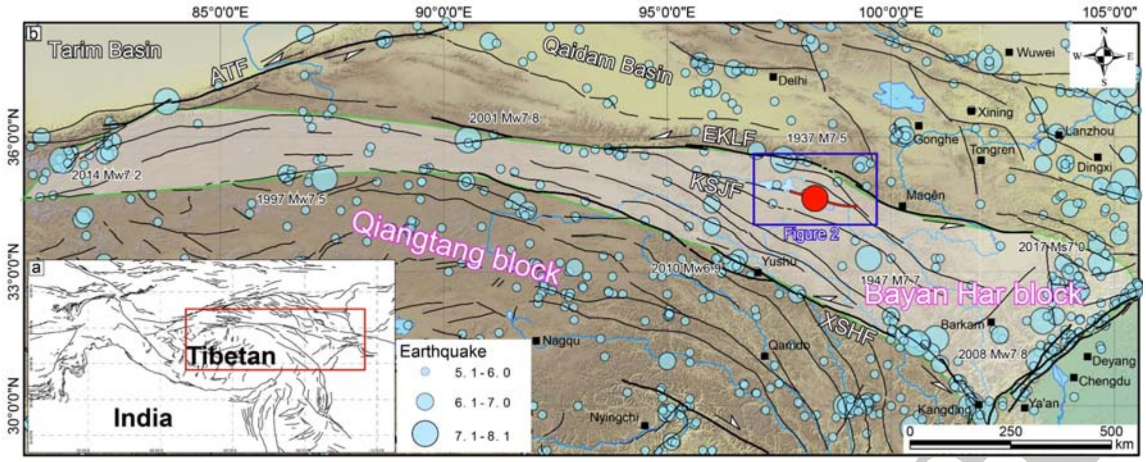

Figure 1 Seismotectonic map around Bayan Har block. The active faults are revised from Deng et al., 2007. The red lines indicate the roughly location of Jiangcuo fault. The red circle shows the ecpicentre of 2021 Maduo earthquake. The green shaded lines indicate the approximate boundary of Bayan Har block. ATF- Altyn Tagh fault; EKLF-East Kunlun Fault; KSJF-Kunlun Shankou-Jiangcuo fault; XSHF-Xianshuihe fault.

1 Geologic background

1.1 Bayan Har block

Since Cenozoic, the continuous collision between the Indian and Eurasia plate results in the expansion and extrusion of the Tibetan plateau to the marginal zone (Molnar and Stock, 2009). Within the plateau, several large-scale suture zones are formed and continuously active. Located at the central of the plateau, the Bayan Har block is bounded by East Kunlun fault, Xianshuihe fault (XSHF), Altyn Tagh fault (ATF) and Longmenshan fault (LMSF), shaping as a triangle (Fig. 1). It is also one of the most active block within China mainland that is indicated by the frequent strong earthquakes in and around the block (Tapponnier et al., 2001; Zhang et al., 2004; Deng et al., 2010; Wen, 2018; Li et al., 2021).

About 2000-km-long East Kunlun fault extends along the north boundary of Bayan Har block striking nearly EW. The Anemaqen restraining bend is composed of Donggei Cuona segment of East Kunlun fault, locating at east of Maduo with convex surface facing to NE (Li et al., 2011). Previous studies show that the geological slip rates of East Kunlun fault decrease from about 11mm/yr to 3-5.5mm/yr eastward (van de Word et al., 2002; Li C. et al., 2004; Li H. et al., 2005; Kirby et al., 2007; Li Ch. et al., 2011; Ren et al., 2013). Six strong earthquakes (M>7.0) occurred along the East Kunlun fault in historical, of which the 2001 Mw 7.8 Kunlun earthquake was the largest one so far and produced a 426-km-long surface rupture (Department of earthquake disaster prevention, State Seismological Bureau, 1995; Seismological Bureau of Qinghai Province, 1999; Xu et al., 2002; Chen et al., 2003; Deng et al., 2003).

The NW-trending sinistral Xianshuihe fault is the south boundary of Bayan Har block. The long-term slip rate of Xianshuihe fault varies from 6mm/yr to 10-13mm/yr (Zhou et al., 1996, 1997; Chevalier et al., 2017; Bai et al., 2018). More than 20 strong earthquakes have appeared along the Xianshuihe fault of which the 2010 Mw 6.9 Yushu earthquake was the latest one. West of Xianshuihe fault, the left-lateral Manyi fault forms part of the southwest boundary of Bayan Har block. The EW-trending Manyi fault has distinct linear trace along which the 1997 Mw 7.5 Manyi earthquake occurred (Molnar and Chen, 1983; Ren and Zhang, 2019).

Longmenshan thrust fault forms the eastern boundary of Bayan Har block striking NE that separates the Bayan Har block and Sichuan basin. Global Positioning System (GPS) studies indicate that the shortening rate of Longmenshan fault is about 2.0mm/yr (Zhang et al., 2008). Due to the relative lower rate, the seismic hazard potential was underestimated before the occurrence of the 2008 Mw 7.8 Wenchuan earthquake.

Besides the large boundary faults, a series of strike-slip faults develop interior of the Bayan Har block, for example the Dari fault, Kunlun Shankou-Jiangcuo fault (KSJF), Maduo-Gande fault (MGF), South Gande fault (SGF) and Changsha Gongma fault (Figs. 1 and 2). Even though the slip rates of these secondary faults were lower than the boundary faults (Xu et al., 2008; Xiong et al., 2010; Yan et al., 2013; Li Ch. et al., 2016; Liu et al., 2021), strong earthquakes occurred inside the Bayan Har block such as 1947 M 7.7 Dari earthquake along Dari fault (Liang et al., 2020).

1.2 Jiangcuo fault

Due to the high altitude, sparsely populated and difficulties for accessing to the fault, the Jiangcuo fault was rarely studies, hence, we know little about the Jiangcuo fault, regarding the geometry, activity and its deformation features etc. Zhang et al (1996) might be the first and the only one reported the Holocene activity of Jiangcuo fault. Field investigation and aerial photos suggested that the Jiangcuo fault was a left-lateral strike-slip fault trending WNW, along which offset landforms developed. At Yematan, the mountain ridge and channels were sinistral displaced about 25m forming a series of fault scarps in the Pleistocene alluvial fans with the vertical offsets of 0.5-2.5m (Zhang et al., 1996). Moreover, fault fracture zone and ground fissures were found at around Jiangning suggesting that the latest paleo-earthquake occurred before 7900a together with the geochronological data (Zhang et al., 1996). When mapping the active faults of China, these works were adopted by Deng et al. (2007) as shown in Figure 2a. Furthermore, Deng et al. (2007) proposed that the Jiangcuo fault could connect with Kunlun Shankou fault (KSF) westward forming the 500-km-long Kunlun Shankou-Jiangcuo fault.

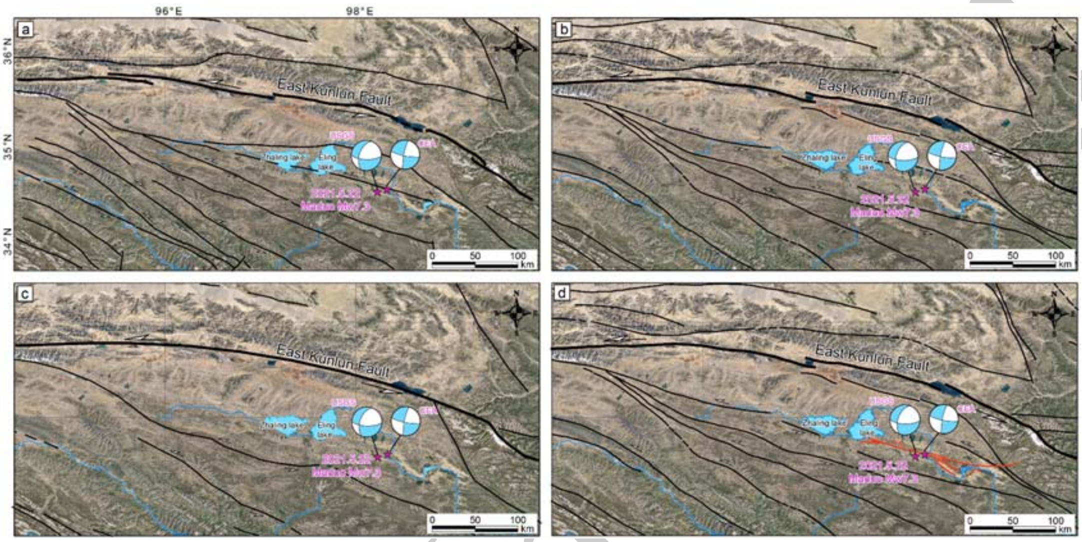

Figure 2 Simple comparison map of active faults around Maduo area. (a) Deng et al., 2007; (b) Xu et al., 2016; (c) Wu et al., 2018; (d) this study. The red lines indicate the extension of Jiangcuo fault.

Although the late Quaternary activity was unraveled in rough by preliminary field investigation (Fig. 3), the detailed geometric features and spatial distribution of Jiangcuo fault is still unknown. Therefore, the Jiangcuo fault was ignored possibly during later active faults mapping projects as shown in Figure 2b (Xu et al., 2016) and Figure 2c (Wu et al., 2018). In this study, we interpreted the spatial distribution of Jiangcuo fault in detail, based on high-resolution satellite image acquired before 2021 Mw 7.3 Maduo earthquake as shown in Figures 2 and 3.

2 Interpretation of Jiangcuo fault

The interpretation of satellite images showed the Jiangcuo fault is 180-km in length, extending from south of Eling lake to east of Changmahe Town, which is the eastern segment of Kunlunshankou-Jiangcuo fault (Fig. 1b). Based on the geometric features of discontinuities, the Jiangcuo fault could be divided into three segments: the western, central and eastern segment, respectively (Fig. 3). The western segment strikes from E-W to NW composed single continuous fault trace, while the eastern segment strikes nearly E-W. The central segment is composed of several branches striking NW.

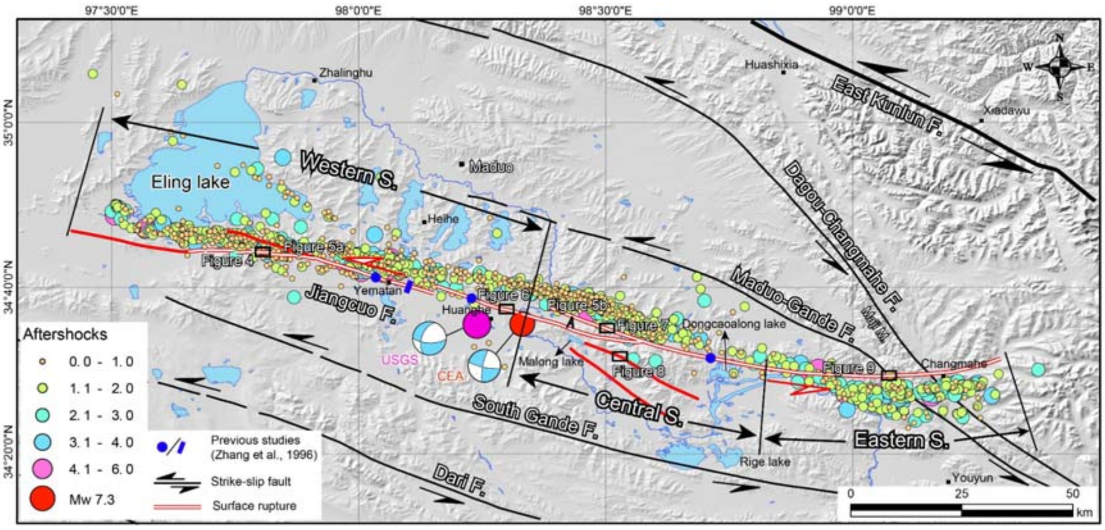

Figure 3 Distribution of active faults at around Maduo region (modified from Deng et al., 2007). The aftershock data cited from Wang et al., 2021. The distribution of surface rupture modified from Li Z. et al. (2021) and Pan et al. (2021). The epicentre and focal mechanism of Mw 7.3 Maduo earthquake comes from U.S. Geological Survey (USGS; big pink circle) and Institute of Geophysics, China Earthquake Adminstration (CEA; big red circle) respectively.

2.1 Western segment

The western segment extends ~75 km as shown in Figure 3 that begins at south of Eling lake and ends at west of Huanghe Town striking nealy E. It can be further divided into two secondary segments from west to east: Eling lake part and Yematan part. The Eling lake part is comprised of two different trending faults that the north branch strikes S70°E extending into the lake and the south branch strikes nearly E-W at south of Eling lake. The two branches converge into one fault striking S70°E roughly, the Yematan part, at southeastern most of Eling lake (Fig. 3). At south of Eling lake, the rivers flow into the lake from south to north. As the basin region, the topographic feature is well shown as low relief mountain, which is mainly occupied by multiple stage alluvial fans at the front of hills.

At Langma village, the Eling lake part of Jiangcuo fault appears as a distinct linear structure on the satellite image (Fig. 4a). We recognized two different alluvial fans at this site: Fan 1 and Fan 2. The Fan 1 was cut and eroded by Fan 2, indicating the relative old age of Fan 1 (Fig. 4b). The swamps present as linear ponds along the fault traces. The apparent left-laterally deflected channel was formed due to a combination of abandonment of original downstream channel and capture of new downstream channel, resulted from the continuous left-lateral motion along the fault (Fig. 4b). Also, the fault has a certain vertical slip component showing with linear scarps along the fault trace (Fig. 4b).

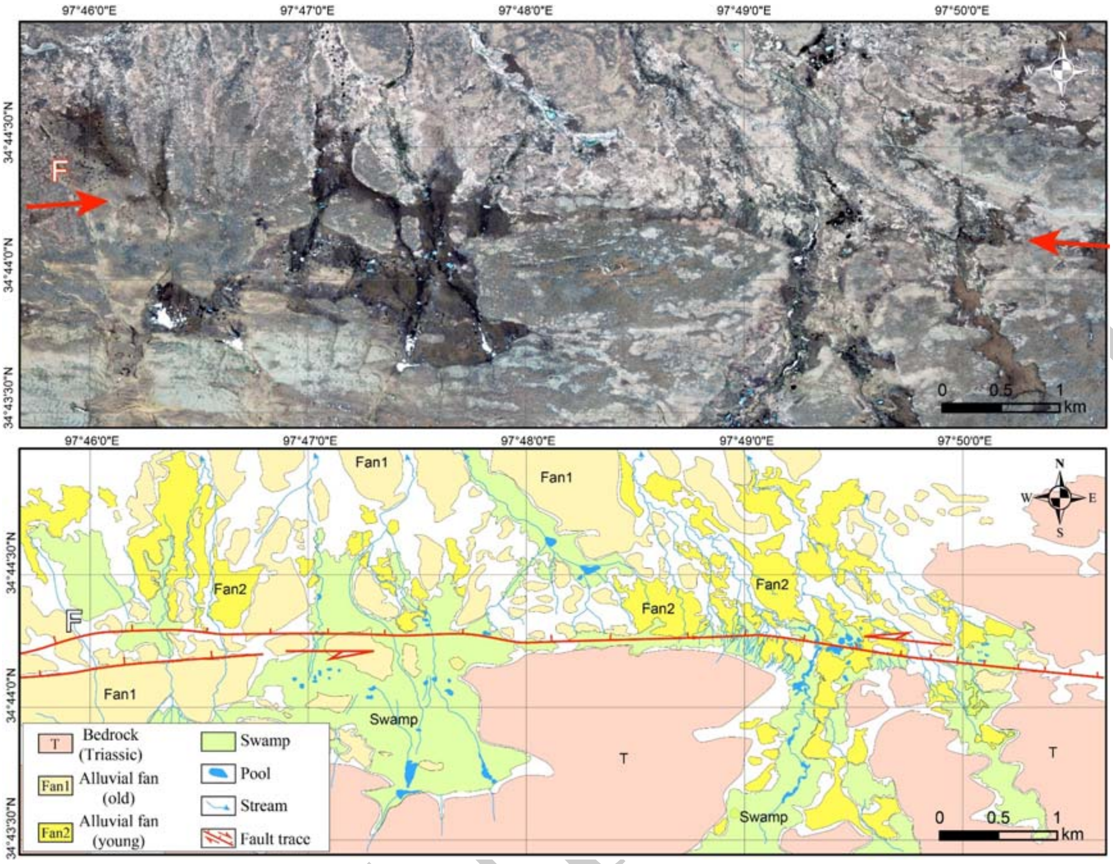

Figure 4 Linear features along the Jiangcuo fault south of Eling lake on the satellite image (a) and its interpretation of the fault trace (b).

To east, the Yematan part extends along the front of Heihe mountain, which separates the mountain and Yematan valley. Owing to the flat terrain within the source of the Yellow River, the Yematan valley is composed of swamp in the center and late Quaternary alluvial fans along the mountain front. The fault trace appears as continuous linear structure in the imagery showing as fault scarps (Fig. 5a). Therefore, the co-seismic deformation is clearly observed along this segment, which is the most obvious coseismic surface rupture of Maduo earthquake (Pan et al., 2021). Located at north of Huhanghe Town, the Jiangcuo fault presents as the sag ponds, beheaded channels, fault valley and left-lateral offset of rivers in the imagery at eastern end of Yematan segment (Fig. 6a). Our interpretation of high-resolution GF-2 images shows that the late Quaternary units is mainly comprised of two alluvial fans distributed in the valley and diuvium fans distributed along the front of hills (Fig. 6b). The swamp spreads linearly along the fault within the sag pond accompanying with the channel offset at east of this site (Fig. 6b).

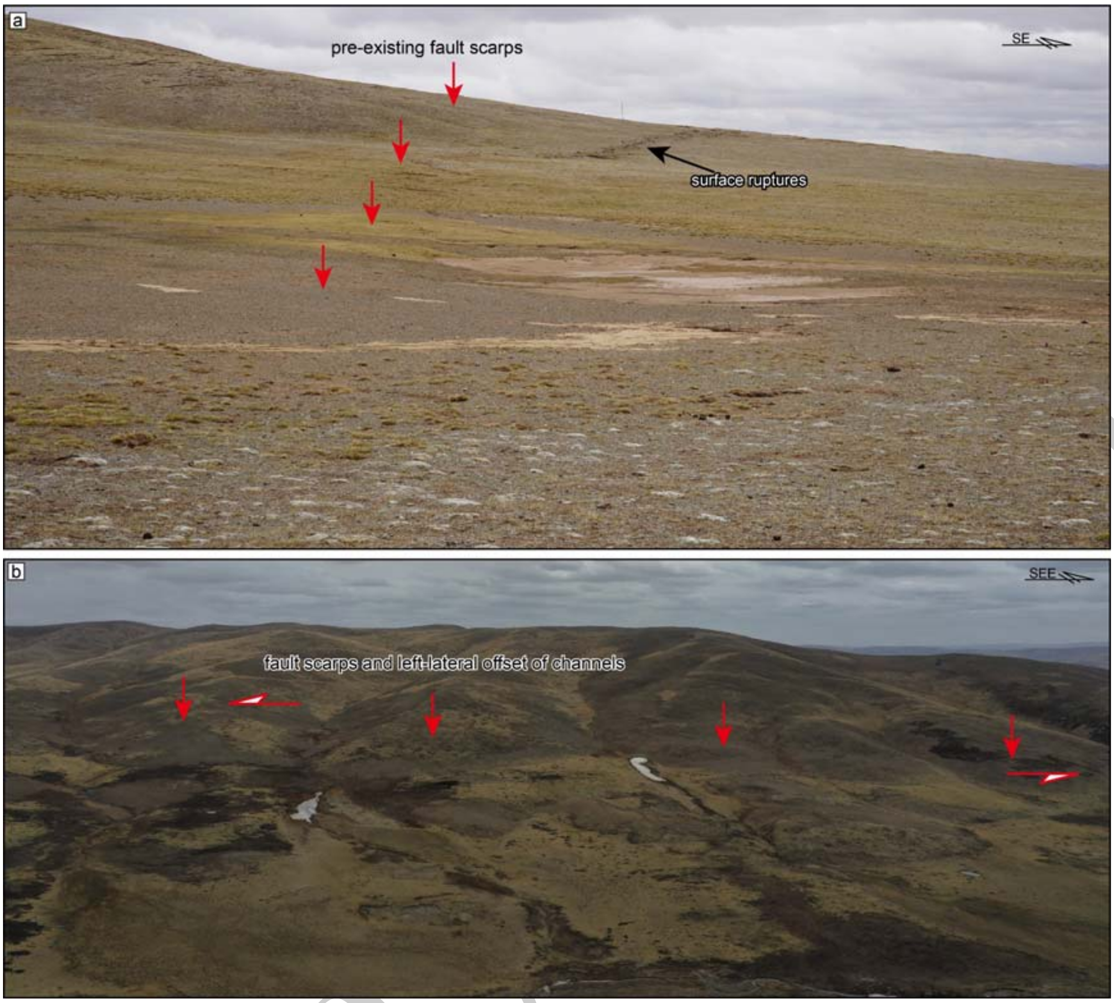

Figure 5 (a) photo of fault scarps developed in late Quaternary units along the western segment of Jiangcuo fault; (b) photo of fault scarps and systematic left-lateral offset of channels along the central segment taken by an unmanned aerial drone.

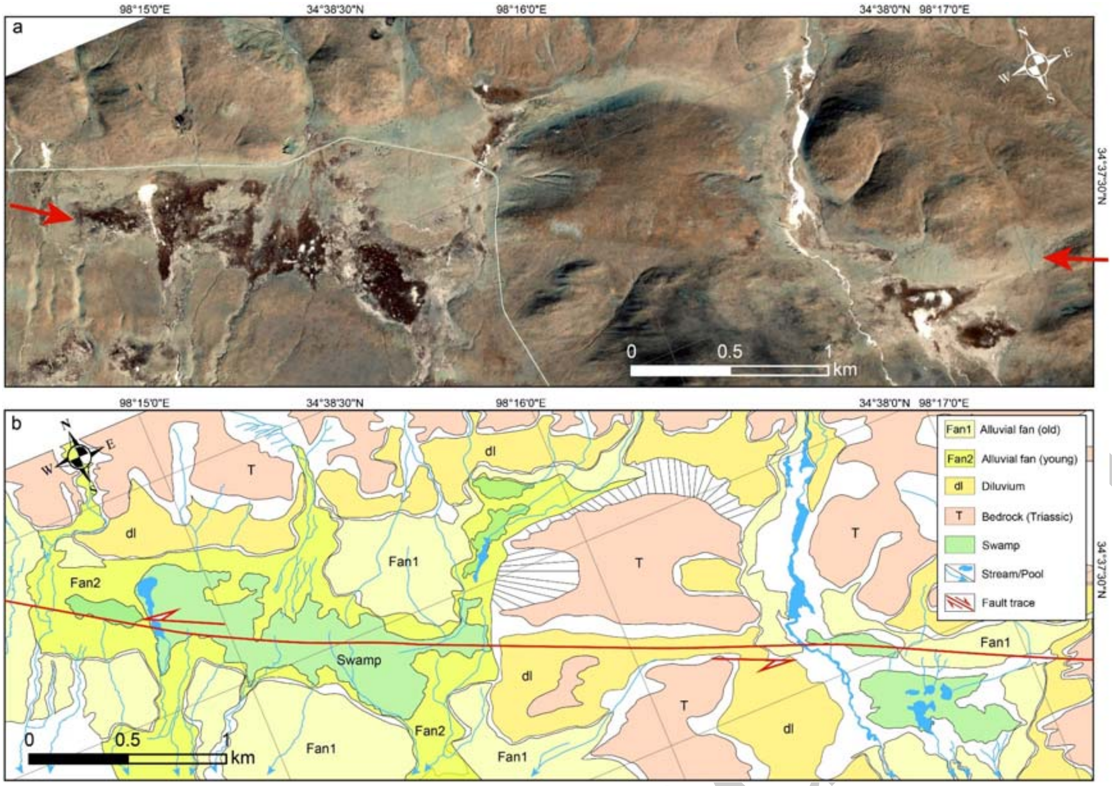

Figure 6 Linear features along Jiangcuo fault at north of Huanghe Town (a) and its interpretation of the fault trace and displaced landforms (b).

2.2 Central segment

The ~55-km-long central segment strikes S70°-80°E. This segment is comprised by several branches which is different from the western and eastern segment (Fig. 3). The north branch, main active one, extends within the mountains appearing as linear fault valleys. At the west, it connects with western segment by fault step over (Fig. 3). By contrast, the fault trace is unclear between the central and eastern segment due to the eolian sands around Dongcaoalong lake possibly. The indistinct fault trace is also similar to the aftershock features of Maduo earthquake that exists a gap at the connection area (Fig. 3; Wang et al., 2021). At 20-km east of Huanghe Town, the Jiangcuo fault presents as clear linear fault valley, scarps and beheaded channels in the imagery (Fig. 7a). Three fractures develop at central part of this site resulting in left-lateral mountain ridges, gullies and linear little sag ponds (Figs. 7b and 7c). To the southeast, the fault scarps and systematic offset of channels also appear along the hill front (Fig. 5b).

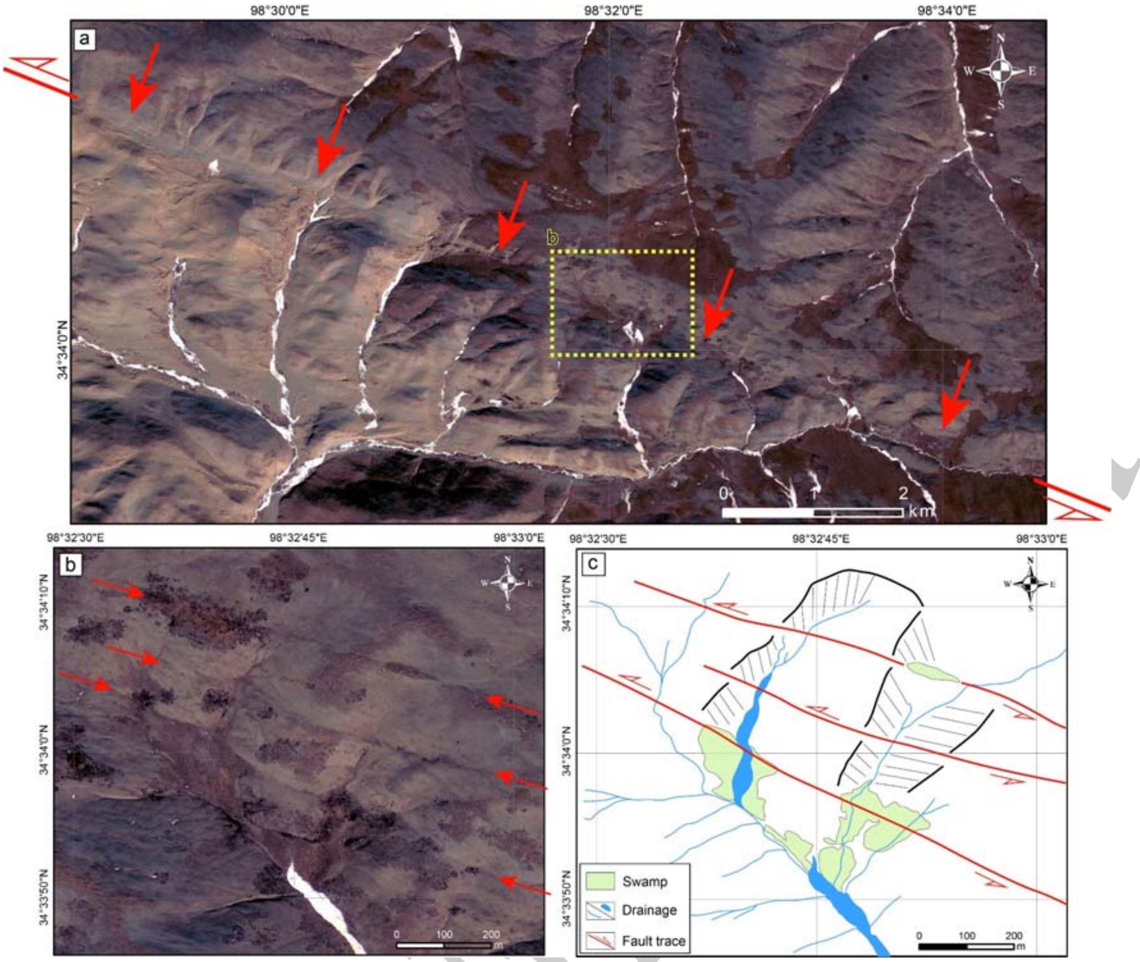

Figure 7 (a) Linear fault valleys along the central part of Jiangcuo fault on the satellite image (GF-2 with resolution <1m); (b&c) Typical faulted landforms and its interpretation.

East of Malong lake, the central branch spreads along the front of Tongbugang mountain striking about S70°E (Fig. 8a). At this site, linear fault valleys, fault scarps and systematic left-lateral displaced channels were observed on the high-resolution satellite image (Fig. 8a). We interpret two terraces along one channel that was displaced by the fault together with the left-lateral ridge and drainage (Figs. 8b and 8c). The geomorphic analyses of high-resolution images show that the channels or ridges have three left-lateral offsets of ~170m, ~65m and ~33m respectively (Fig. 8c), which represent the accumulative displacement.

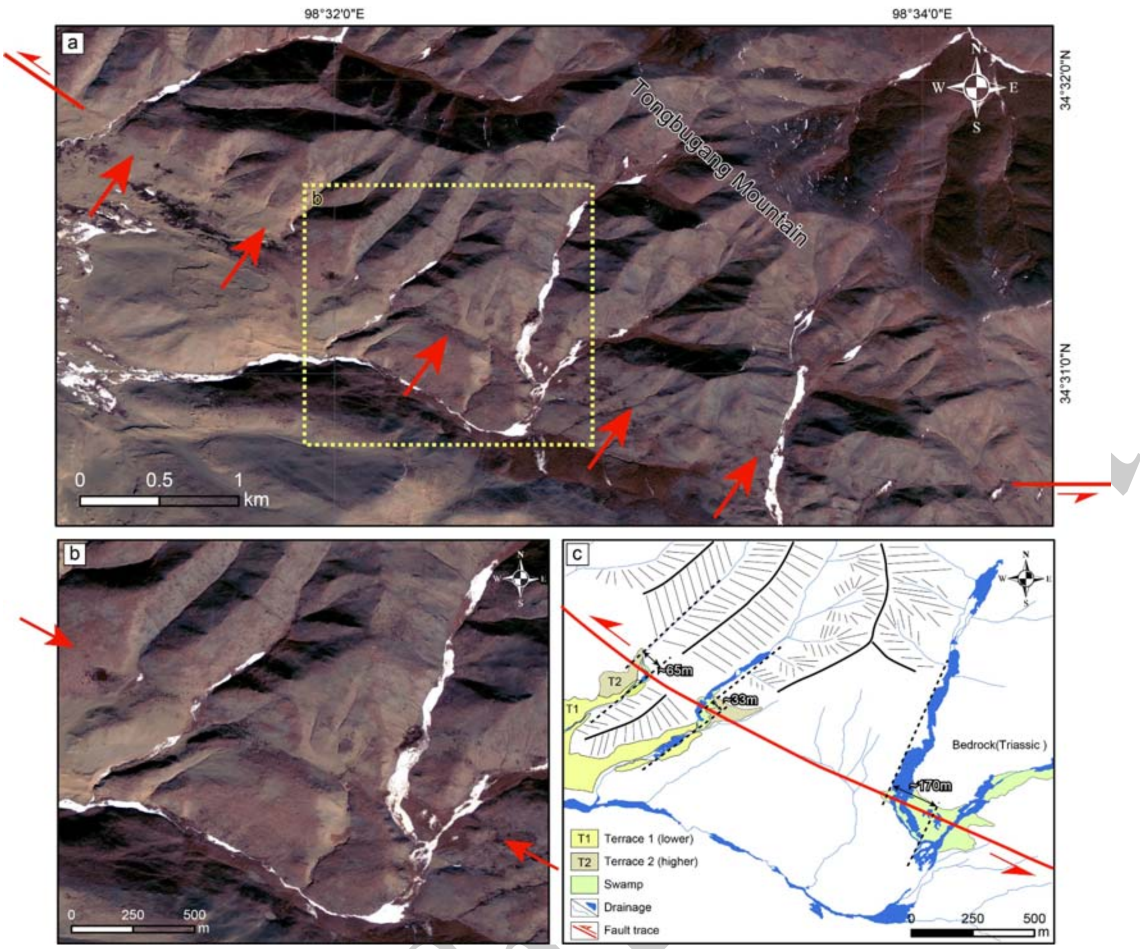

Figure 8 (a) Linear fault valleys along the Jiangcuo fault at west of Huanghe Town. (b&c) The consistent left-lateral offset of gullies on the satellite image and its interpretation.

Northwest of the Rige lake, the ~25-km-long south branch extends parallel to the Yellow river striking about N120°E (Fig. 3). It separates the late Quaternary eolian sands to the north with the alluvial and proluvial fans to the south appearing distinct linear structure (Geological brigade of regional geological survey in Qinghai Province, 1992).

2.3 Eastern segment

The 50-km-long eastern segment strikes nearly N80°-110°E cutting cross the Maji Mountain and Maduo-Gande fault and Dagou-Changmahe fault (Fig. 3). Most of the eastern segment spreads within bedrocks showing as fault valleys and systematic left-lateral offset of gullies.

The Jiangcuo fault intersects with the Maduo-Gande fault with about 45° at 10-km west of Changmahe Town (Figs. 9a and b). At this site, the trending of Jiangcuo fault transforms from N100°E to N80°E (Fig. 9b) presenting as fault valleys (Fig. 10a and b) and displacements of channels (Fig. 9b). Different with the Jiangcuo fault, the Maduo-Gande fault strikes about N30°W located at the front of hills (Fig. 9a). Our interpretation of imagery shows that systematic displacement of channels appears along the Maduo-Gande fault as well as the beheaded gullies (Fig. 9b).

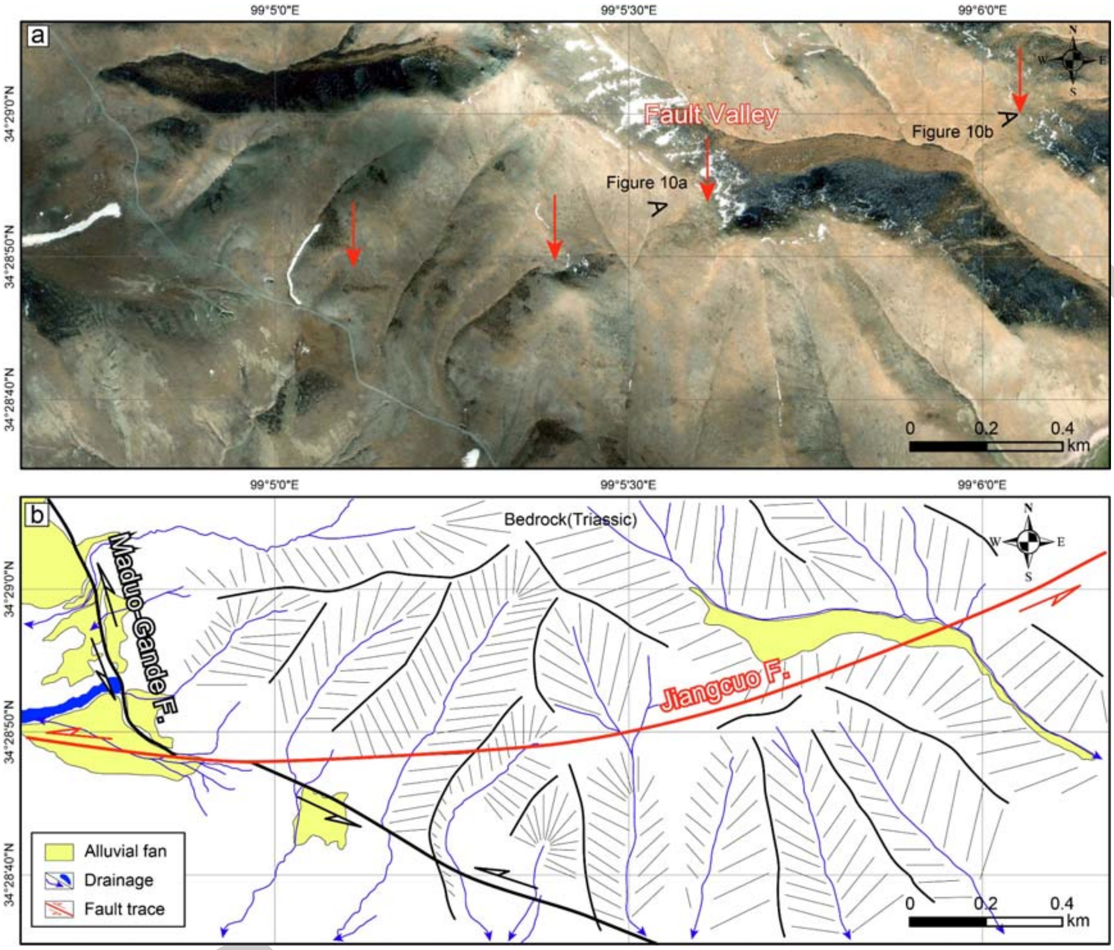

Figure 9 Linear features along the Jiangcuo fault at west of Changmahe Town on the satellite image (resolution 1.2m; a) and the interpretations (b).

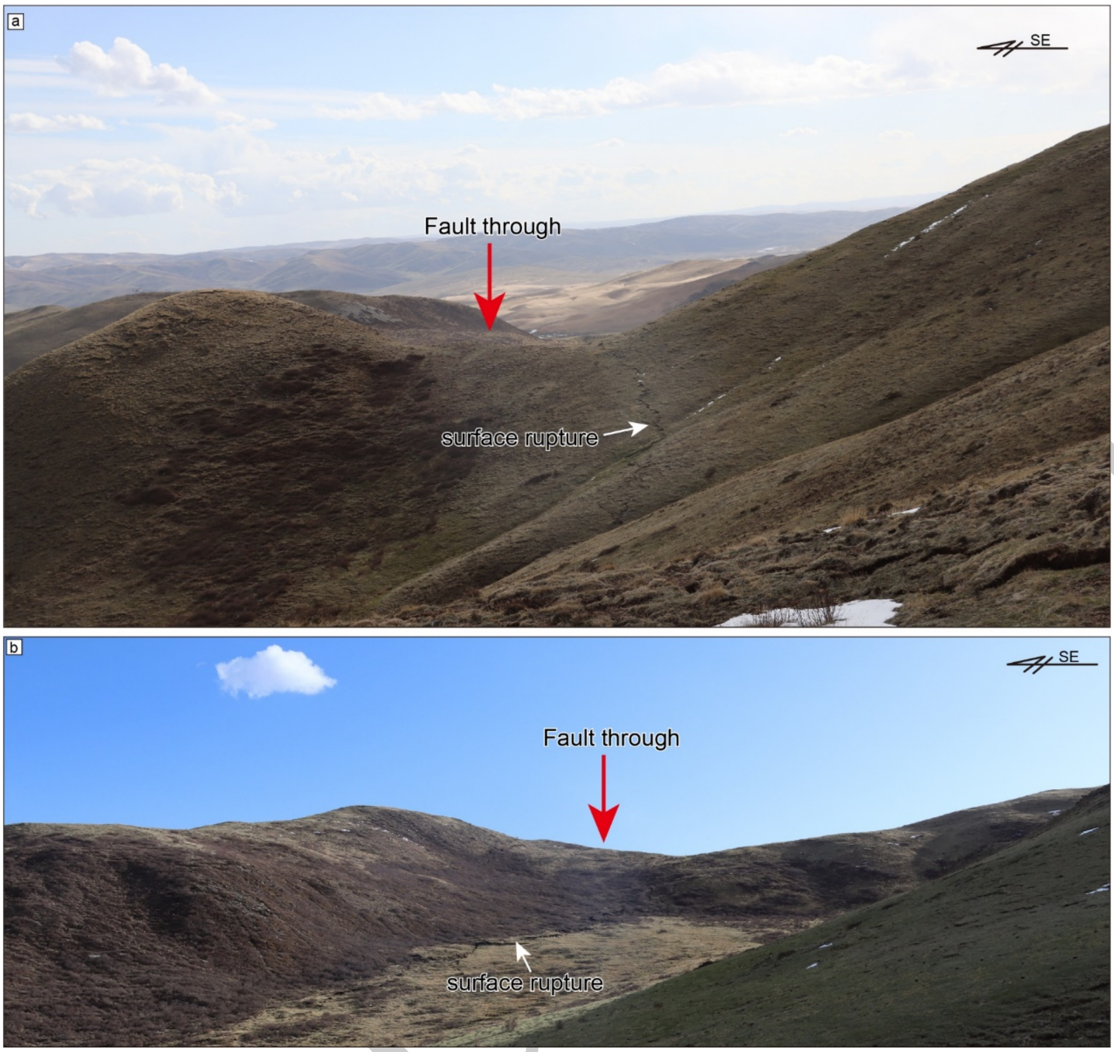

Figure 10 Fault valleys along the Jiangcuo fault at west of Changmahe Town with the position showing in Figure 9a.

3 Discussion

The central to eastern East Kunlun fault is composed of Donggei Cuona, Maqin and Maqu segments, where the Donggei Cuona and Maqin segments strike S75°-80°E forming a restraining bend at the transition zone named as Anemaqen bend (AB). The mountain uplift and crust shortening occurred within the Anemaqen bend shaped the Anemaqen Mountain (Cunningham, 2007). Similarly, the arc Dagou-Changmahe fault extends along the southwestern margin of Anemaqen paralleling to the East Kunlun fault at Donggei Cuona and later to Anemaqen bend (Fig. 2d). Experiment of rock mechanics and simulation of bend faults suggested that the restraining bend or step would restrain or stop the spreading of slips of one fault (Ma et al., 2008). Due to the existing of Anemaqen bend, the left-lateral strain of Donggei Cuona segment could not spread to Maqin totally before the rupture of Anemaqen bend. Then, a series of secondary faults would appear to absorb the accumulative strain at around Anemaqen bend. Field investigation of surface rupture suggested that the Jiangcuo fault was the earthquake structure of Maduo earthquake (Li et al., 2021; Pan et al., 2021) which was consistent with the aftershock distribution (Wang et al., 2021). Westward, the Jiangcuo fault connected with Kunlun Shankou fault—— a subbranch of East Kunlun fault, which was ruptured during the 2001 Kunlun Mw 7.9 earthquake (Deng et al., 2007; Chen et al., 2003; Lin et al., 2011). The Jiangcuo fault developed east to the Kunlun Shankou fault which could connected with it. Therefore, we suggest that the Dagou-Changmahe fault, Maduo-Gande fault and Jiangcuo fault could be branches of East Kunlun fault, all of which forms a wide boundary between the Bayan Har block and Qaidam block.

Several seismic studies have revealed the deep structure around Maduo area crossed the East Kunlun fault. The teleseismic receiever-function and wide—angle seismic profiles near Golmud indicated that the East Kunlun fault dipped northward with the angle ~70° at a depth of 60km and did not cut the Moho (Vergne et al., 2002; Karplus et al., 2010). Although the East Kunlun fault displaces the Moho near Maduo, the geometry is complex. Wang et al. (2011) reanalyzed Maduo section based on the work of Vergne et al. (2002) and suggested that a zone of north-dipping and south-dipping thrusts duplicated the Moho vertically and the secondary faults within Bayan Har block converged into the East Kunlun fault at the depth of ~60km. Recently, a magnetotelluric profile across Jiangcuo fault and East Kunlun fault suggests that there exists a strong bulge deformation of high conductivity layer (HCL) interior of middle and lower crust below Jiangcuo fault and Dagou-Changmahe fault (Zhan et al., 2021). The deformation of HCL indicates that the Jiangcuo fault and other secondary faults absorb the left-lateral slip of East Kunlun fault and the shortening under NE-SW compress.

Based on the geometric analysis of East Kunlun fault and Jiangcuo fault as well as the structures in depth, we interpret that the Jiangcuo fault is one subbranch of East Kunlun fault as well as the Maduo-Gande fault and Dagou-Changmahe fault, all of which constitute a wide fault zone together with Kunzhong fault north of East Kunlun fault. The boundary zone between Bayan Har block and Qaidam block named Kunlun Belt, became a wider boundary zone near Maduo County, which is illustrated and shown in Figure 11 (Fig. 11).

Six strong earthquakes occurred along the East Kunlun fault leaving two rupture gaps without historical earthquakes in record: Xidatan segement and Maqin-Maqu segment (Fig. 12; van der Woerd et al., 2002; Wen et al., 2007; Li Ch. et al., 2011). Paleo-earthquake studies indicated that the elapse time of the last earthquake event had exceeded or approached its recurrence period (Li Ch. et al., 2011). The Maqin-Maqu segment faces a high seismic risk that is consistent with the study of magnetotelluric profiles (Pan et al., 2021; Zhan et al., 2021). Additionally, the surface rupture of 2001 Kunlun earthquake ended at the western most of Kunlun Shankou-Jiangcuo fault resulting in a rupture gap along the Kunlun Shankou-Jiangcuo fault. The occurrence of the 2021 Maduo earthquake ruptured the eastern part of Kunlun Shankou-Jiangcuo fault leaving the western segment as rupture gap on the East Kunlun fault (Fig. 12). Therefore, both rupture gaps overlie on the East Kunlun fault now. Although the mechanics of rupture gap remains unclear, the strong earthquake risks along the East Kunlun fault should be given enough attention in the future, especially the rupture gap region between the 2001 Kunlun, 1937 Huashixia and 2021 Maduo earthquakes.

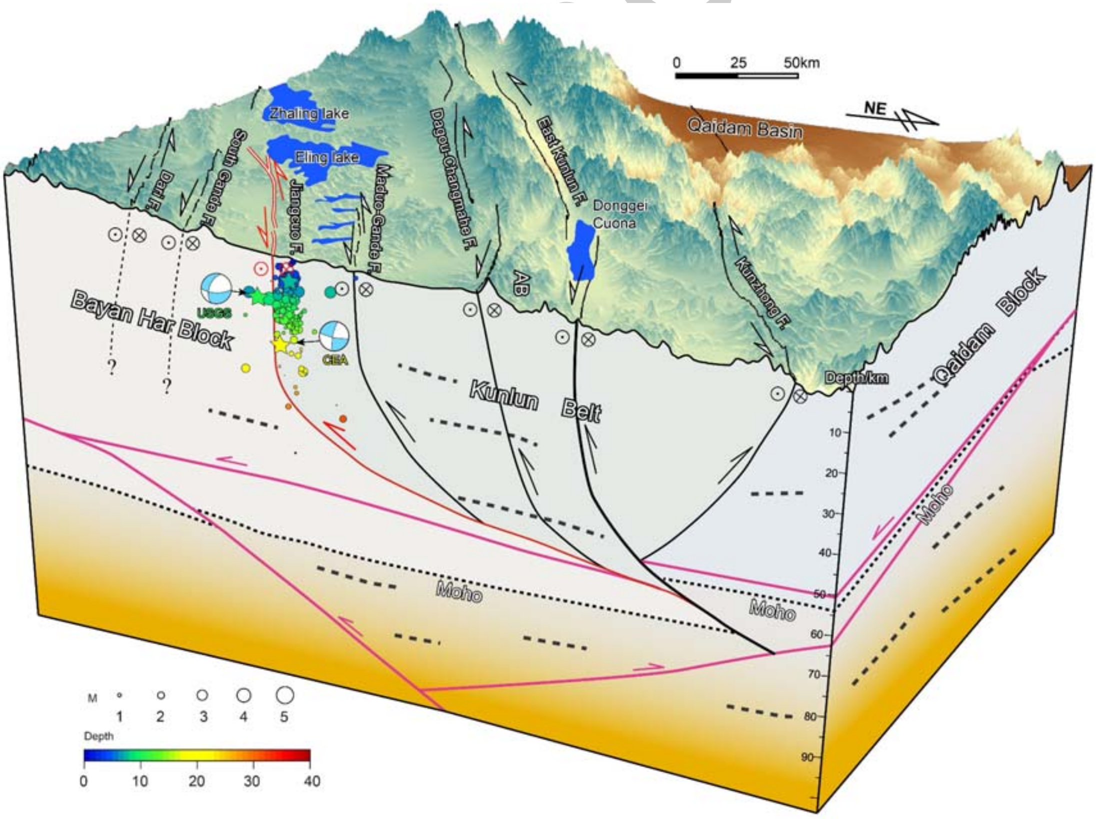

Figure 11 Simple 3D seismogenic structure of the Jiangcuo fault and its relationship with the Kunlun fault zone. The deep structures modified from Wang et al. (2011). The stars show the depth of main shock of Maduo earthquake. The aftershocks are cited from Wang et al. (2021). AB- Anemaqen bend

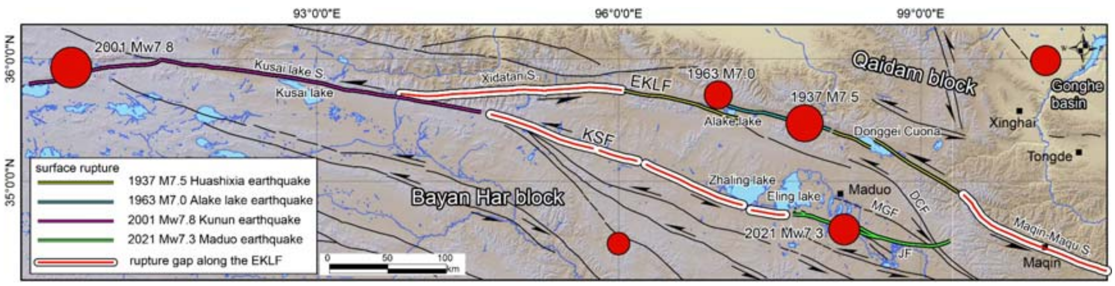

Figure 12 Abridged diagram of surface rupture distribution of four strong earthquakes and rupture gaps along East Kunlun fault. The active faults revised from Xu et al., 2016. The distribution of surface ruptures modified from Chen et al., 2003, Guo et al., 2007, Li Z. et al., 2021 and Pan et al., 2021.

Previous studies stated that the probality of earthquake occurrence on one fault was not independent of another and the earthquake interaction was a fundamental feature of seismicity, resulting in earthquake sequences, clustering and aftershocks (Stein, 1999). The Coulomb stress transfer is a manner of understanding the earthquake occurrence, interaction and probabilistic hazard which are widely used in evaluating seismic potentials (e.g., Stein et al., 1997; Stein, 1999; Kilb et al., 2002; Toda et al., 2002; Xiong et a., 2010, 2015). For one large earthquakes, the stress would be released along the rupture and transferred at the rupture tips and off the fault. Due to the stress transfer, earthquakes would migrate along the fault and trigger other moderate to strong earthquakes adjacent, which was used in many giant faults e.g., North Anatolian fault (Stein et al., 1997) and Longmenshan fault (Xu et al., 2017). Similarly, numerical results suggested a good correlation between the stress transfer, accumulation and earthquakes occurrence along the main East Kunlun fault, and the Xidatan segment and Maiqn-Maqu segment have the high level of stress accumulated after 2001 Kunlun earthquake and 1937 Huashixia earthquake (Xiong et al., 2010). Viewed in this light, the stress of Kunlun Shankou fault locating at the east of Kusai lake segment, would increase as a result of 2001 Kunlun earthquake. Also, the 2021 Maduo earthquake would change the stress pattern of Kunlun Shankou-Jiangcuo fault and East Kunlun fault loading stress to KSF and Maqin-Maqu segment. Therefore, we suggest that the Kunlun Shankou fault would confront with high potential earthquake hazard as well as Xidatan and Maqin-Maqu segments along the main East Kunlun fault.

4 Conclusion

Detailed interpretation of high-resolution images shows that the Jiangcuo fault is 180-km in length, striking nearly E extending from Eling lake to Changmahe town, connecting eastward to the Kunlun Shankou fault, which is the seismogenic fault of the 2021 Maduo Mw 7.3 earthquake. Based on the geometric features, the Jiangcuo fault could be divided into three segments appearing as the linear structures, fault valleys, scarps and systematic offset of channels. Geometric analysis and deep lithosphere structure around Maduo County suggest that the Jiangcuo fault should be a subbranch of East Kunlun fault to the south. The Kunlun fault belt is composed of East Kunlun fault and several branch faults around Anemaqen Mountain, including the Jiangcuo fault. The boundary between Bayan Har block and Qaidam block is presented as a wide deformation zone near Maduo County. Our studies also indicate that there are two main rupture gaps along the Kunlun fault belt after the occurrence of the 2021 Maduo earthquake. One rupture gap is along the western Kunlun Shankou-Jiangcuo fault and the other one is along the main East Kunlun fault between the 2001 Kunlun, 1937 Huashixia and 2021 Maduo earthquakes. Due to the positive stress transfer studies, since the 1937 Hushixia earthquake, these two rupture gap is continuously receiving increase stress rate resulted from the 1937 Hushixia, 2001 Kunlun and 2021 Maduo earthquakes. Although the two rupture gaps exist on two faults, but the two faults are sub-branches of the East Kunlun fault zone. Hence, we propose that the strong seismic potential of the western Kunlun Shankou-Jiangcuo fault and Xidatan fault should be given enough attention in the future.

ACKNOWLEDGEMENTS

This work was supported by National Nonprofit Fundamental Research Grant of China, Institute of Geology, China, Earthquake Administration (Grants No. IGCEA1803; IGCEA2110) and the Seismic Hazard Prevention Project from Ministry of Finance (Grant No. JH-21-10).

REFERENCES CITED

Bai, M., Chevalier, M.-L., Pan, J., et al. 2018. Southeastward increase of the late Quaternary slip-rate of the Xianshuihe fault, eastern Tibet. Geodynamic and seismic hazard implications. *Earth and Planetary Science Letters*, 485, 19-31.

Chen, J., Chen, Y., Ding, G., et al. 2003. Surface rupture zones of the 2001 earthquake Ms 8.1 west of Kunlun Pass, Northern Qinghai-Xizang plateau. *Quaternary Sciences*, 23(6), 629-639. (in Chinese with English abstract)

Chevalier, M.-L., Leloup, P. H., Replumaz, A., et al. 2017. Temporally constant slip rate along the Ganzi fault, NW Xianshuihe fault system, eastern Tibet. *GSA Bulletin*. 130(3/4): 396-410

China Earthquake Networks Center. 2021. https://news.ceic.ac.cn/CC20210522020411.html.

Cunningham, W. 2007. Teconics of Strike-Slip Restraining and Releasing Bends. In (Vol. 290, pp. 1-12).

Deng, Q., Gao, X., Chen, G., et al. 2010. Recent tectonic activity of Bayankala fault block and the Kunlun Wenchuan earthquake series of the Tibetan Plateau. *Earth Science Frontiers*, 15(5), 163-178. (in Chinese with English abstract)

Deng, Q., Ran, Y., Yang, X., et al. 2007. Active tectonic map of China. (in Chinese)

Deng, Q., Zhang, P., Ran, Y., et al. 2003. Active tectonics and earthquake activities in China. *Earth Science Frontiers*, S1, 66-73. (in Chinese with English abstract)

Department of Earthquake Disaster Prevention of State Seismological Bureau. 1995. The catalogue of historical strong earthquakes in China. Seismological Press Beijing, 1-514. (in Chinese)

Geological brigade of regional geological survey in Qinghai Province, 1992. Geological map of the Republic of China (1:200000 Hegesi sheet)

Guo, J., Lin, A., Sun, G., et al. 2007. Surface Ruptures Associated with the 1937 M 7.5 Tuosuo Lake and the 1963 M 7.0 Alake Lake Earthquakes and the Paleoseismicity along the Tuosuo Lake Segment of the Kunlun Fault, Northern Tibet. *Bulletin of the seismological Society of America*, 97(2), 474-496.

Karplus, M. S., Zhao, W., Klemperer, S. L., et al. 2011. Injection of Tibetan crust beneath the south Qaidam Basin: Evidence from INDEPTH IV wide-angle seismic data. *Journal of Geophysical Research*, 116(B7): 1-23.

Kilb, D., Gomberg, J., & Bodin, P. 2002. Aftershock triggering by complete Coulomb stress changes. Journal of Geophysical Research: Solid Earth, 107(B4), ESE 2-1-ESE 2-14.

Kirby, E., Harkins, N., Wang, E., et al. 2007. Slip rate gradients along the eastern Kunlun fault. *Tectonics*, 26(2): 1-16.

Li, C., He, Q., & Zhao, G. 2004. Holocene slip rate along the eastern segment of the Kunlun fault. *Seismology and Geology*, 26(4), 122-133. (in Chinese with English abstract)

Li, C., Xu, X., Wen, X., et al. 2011. Rupture segmentation and slip partitioning of the mid-eastern part of the Kunlun fault, north Tibetan Plateau. *Science China Earth Sciences,* 41(9), 12-13. (in Chinese with English abstract)

Li, C., Yuan, D., Yang, H., et al. 2016. The Tectonic Activity Characteristics of Awancang Fault in the Late Quaternary, the Sub-Strand of the Eastern Kunlun Fault. *Seismology and Geology*, 38(1), 44-64. (in Chinese with English abstract)

Li, H., Pan, J., Sun, Z., et al. 2021. Continental tectonic deformation and seismic activity: a case study from the Tibetan Plateau. *Acta Geologica Sinica*, 95(1), 194-213. (in Chinese with

English abstract)

Li, H., Van der Woerd, J., Tapponnier, P., et al. 2005. Slip rate on the Kunlun fault at Hongshui Gou, and recurrence time of great events comparable to the 14/11/2001, Mw~7.9 Kokoxili earthquake. *Earth and Planetary Science Letters*, 237, 285-299.

Li, Z. M., Xu, Y. R., Li, T., et al., 2021. Preliminary investigation on Seismogenic structure and surface rupture of Maduo Ms7.4 earthquake on May 22, 2021, Qinghai Province. *Seismology and Geology,* Accepted. (in Chinese with English abstract)

Liang, M., Yang, Y., Du, F., et al. 2020. Late Quaternary activity of the central segment of the Dari Fault and restudy of the surface rupture zone of the 1947 M7 3/4 Dari earthquake, Qinghai province. *Seismology and Geology,* 42(03), 703-714. (in Chinese with English abstract)

Lin, A., & Nishikawa, M. 2011. Riedel shear structures in the co-seismic surface rupture zone produced by the 2001 Mw 7.8 Kunlun earthquake, northern Tibetan Plateau. *Journal of Structural Geology*, 33(9), 1302-1311.

Liu, L., Li, Y., Zhu, L., et al. 2021. Influence of the 1947 Dari Ms7.7 earthquake on stress evolution along the boundary fault of the Bayan Har block: insights from numerical simulation. *Chinese Journal of Geophysics,* 64(7), 2221-2231. (in Chinese with English abstract)

Ma, S., Chen, S., Liu, P., et al. 2008. Experimental study on the effect of fault step on sliding behavior. *Science China Earth Sciences*, 38(7), 842-851. (in Chinese)

Molnar, P., & Chen, W. P. 1983. Focal depths and fault plane solutions of earthquakes under the Tibetan Plateau. *Journal of Geophysical Research Solid Earth*, 88(B2), 1180–1196.

Molnar, P., & Stock, J. M. 2009. Slowing of India's convergence with Eurasia since 20 Ma and its implications for Tibetan mantle dynamics. *Tectonics*, 28(3), TC3001.

Pan, J., Bai, M., Li, C., et al. 2021. Coseismic surface rupture and seismogenic structure of the 2021- 05- 22 Maduo (Qinghai) Ms7.4 earthquake. *Acta Geologica Sinica*, 95(06), 1655-1670. (in Chinese with English abstract)

Ren, J., Xu, X., Yeats, R., et al. 2013. Millennial slip rates of the Tazang fault, the eastern termination of Kunlun fault: Implications for strain partitioning in eastern Tibet. *Tectonophysics*, 608(1), 1180-1200.

Ren, Z., & Zhang, Z. 2019. Structural analysis of the 1997 Mw 7.5 Manyi earthquake and the kinematics of the Manyi fault, central Tibetan Plateau. *Journal of Asian Earth Sciences*, 179, 149-164.

Seismological Bureau of Qinghai Province, Institute of Crustal Dynamics of China Earthquake Administration. 1999. Eastern Kunlun Active Fault Zone. Beijing: Seismological Press,1-227. (in Chinese)

Stein, R. S. 1999. The role of stress transfer in earthquake occurrence. *Nature*, 402(6762), 605-609.

Stein, R. S., Barka, A. A., & Dieterich, J. H. 1997. Progressive failure on the North Anatolian fault since 1939 by earthquake stress triggering. *Geophysical Journal International*, 128(3), 594-604.

Tapponnier, P., Ryerson, F. J., Van der Woerd, J., et al. 2001. Long-term slip rates and characteristic slip: keys to active fault behaviour and earthquake hazard. Comptes Rendus de l'Académie des Sciences - Series IIA - *Earth and Planetary Science*, 333(9), 483-494.

Toda, S., Stein, R. S., & Sagiya, T. 2002. Evidence from the ad 2000 Izu islands earthquake swarm that stressing rate governs seismicity. *Nature*, 419(6902), 58-61.

Van Der Woerd, J., Tapponnier, P., Ryerson, F., et al. 2002. Uniform postglacial slip-rate along the central 600 km of the Kunlun Fault (Tibet), from ^{26}Al, ^{10}Be, and ^{14}C dating of riser offsets, and climatic origin of the regional morphology. *Geophysical Journal International*, 148(3), 356-388.

Vergne, J., Wittlinger, G., Hui, Q., et al. 2002. Seismic evidence for stepwise thickening of the crust across the NE Tibetan Plateau. *Earth and Planetary Science Letters*, 203, 25-33.

Wang, C., Gao, R., Yin, A., et al. 2011. A mid-crustal strain-transfer model for continental deformation: A new perspective from high-resolution deep seismic-reflection profiling across NE Tibet. *Earth and Planetary Science Letters*, 306(3-4), 279-288.

Wang, W., Fang, L., Wu, J., et al. 2021. Aftershock sequence relocation of the 2021 MS7.4 Maduo Earthquake, Qinghai, China. *Science China Earth Sciences*, 51(07), 1193-1202. (in Chinese with English abstract)

Wen, X. 2018. The 2008 Wenchuan, 2013 Lushan and 2017 Jiuzhaigou earthquakes, Sichuan, in the last more than one thousand years of rupture history of the eastern margin of the Bayan Har block. *Acta Seismologica Sinica*, 40(3), 4-16. (in Chinese with English abstract)

Wu, Z., Zhou, C., Ma, X., et al. 2018. Distribution map of active faults in China and its adjacent sea area. (in Chinese)

Xiong, R., Ren, J., Zhang, J., et al. 2010. Late quaternary active characteristics of the Gande segment in the Maduo-Gande fault zone. *Earthquake*, 30(4), 65-73. (in Chinese with English abstract)

Xiong, W., Tan, K., Liu, G., et al. 2015. Coseismic and postseismic Coulomb stress changes on surrounding major faults caused by the 2015 Nepal M_W7.9 earthquake. *Chinese Journal of Geophysics*, 58(11), 4305-4316. (in Chinese with English abstract)

Xu, J., Shao, Z. G., Liu-Zeng, J., et al. 2017. Analysis of interaction between great earthquakes in the eastern Bayan Har block based on changes of Coulomb stress. *Acta Geophysica Sinica*, 60, 4056-4068. (in Chinese with English abstract)

Xu, X., Chen, W., Yu, G., et al. 2002. Characteristic Features of the Hoh Sai Hu (Kunlunshan) Earthquake (Ms8.1), Northern Tibetan Plateau, China. *Seismology and Geology*, 24(1), 1-13. (in Chinese with English abstract)

Xu, X., Han, Z., Yang, X., et al. 2016. Seismotectonic map of China and adjacent areas. (in Chinese)

Xu, X., Wen, X., Chen, G., et al. 2008. Discovery of the Longriba fault zone in eastern Bayan Har block, China and its tectonic implication. *Science in China Series D: Earth Sciences*, 51(9), 1209-1223. (in Chinese with English abstract)

Yan, L., Li, Y., Zhao, G., et al. 2013. Study on the Late Quaternary Activity Characteristics and its Tectonic Geomorphology Response of the middle Segment of Dari Fault in the Northeastern Tibetan Plateau. *Acta Geologica Sinica*, 87(z1), 403-405. (in Chinese with English abstract)

Zhan, Y., Liang, M., Sun, X., et al. 2021. Deep structure and seismogenic pattern of the 2021.5.22 Madoi (Qinghai) Ms7.4 earthquake. *Chinese Journal of Geophysics*, 64(07), 2232-2252. (in Chinese with English abstract)

Zhang, P.-Z., Shen, Z., Wang, M., et al. 2004. Continuous deformation of the Tibetan Plateau from global positioning system data. *Geology*, 32(9), 809.

Zhang, P., Xu, X., Wen, X., et al. 2008. Slip rates and recurrence intervals of the Longmen Shan active fault zone, and tectonic implications for the mechanism of the May 12 Wenchuan earthquake, 2008, Sichuan, China. *Chinese Journal of Geophysics*, 51(4), 1066-1073. (in Chinese with English abstract)

Zhang, Y., Li, M., Meng, Y., et al. 1996. Research on fault activities and their seismogeological implication in Bayankala Mountain area. *Research on Active Faults*, 5, 154-171. (in Chinese with English abstract)

Zhou, R., Ma, S., & Cai, C. 1996. Late Quaternary active features of the Ganzi-Yushu fault zone. *Earthquake Research in China*, 12(3), 250-260. (in Chinese with English abstract)

Zhou, R., Wen, X., Cai, C., et al. 1997. Recent earthquakes and assessment of seismic tendency on the Ganzi-Yushu fault zone. *Seismology and Geology*, 19(2), 20-29. (in Chinese with English abstract)